ΑΔΣ

Advances in Decision Sciences

Michael McAleer

Editor-in-Chief
University Chair Professor
Asia University, Taiwan

Opinion Dynamics and Disagreements on Financial Networks[*]

Monica Billio[**]
University Ca' Foscari of Venice

Roberto Casarin
University Ca' Foscari of Venice

Michele Costola
SAFE, House of Finance, Goethe University Frankfurt

Lorenzo Frattarolo
University Ca' Foscari of Venice

Revised: November 2019

[**]Corresponding author: `billio@unive.it`.

Abstract

We propose a new measure of disagreement based on connectedness, which generalizes the disagreement index introduced in Billio et al. (2018). Building on the lifting approach in Hendrickx (2014), we extend Billio et al. (2018) to signed networks, which allows us to consider more general consensus dynamics and disagreement with antagonistic behaviour. Synthetic and real-world financial networks of serial correlation are considered for illustrating the new measure and for studying opinion dynamics and convergence to consensus on prices for financial assets.

Keywords: Consensus dynamics; Disagreement; Financial contagion; Financial Networks; Graph Theory, Opinion Dynamics.

JEL: C58; D83; D85; G12; G29.

1 Introduction

Given the threat to financial stability and the real economy, quantifying systemic risk is now investigated by scholars as well as policy makers. More recently, graph theoretic measures and in particular convergence of agents on a network to a consensus have been involved in the systemic risk analysis and in the construction of early warning indicator for banking crises (Billio et al., 2018). Financial networks are usually extracted by testing for significant correlations (e.g., see Bianchi et al., 2019), and for Granger (e.g., see Ahelegbey et al., 2016a,b; Billio et al., 2019b) or Sims causality (e.g., see Diebold and Yılmaz, 2014; Diebold and Yilmaz, 2015) between time series of returns. In this paper, we propose a generalization of the disagreement index of Billio et al. (2018). Building on the lifting approach in Hendrickx (2014), we extend the results in Billio et al. (2018) to signed networks. This allows us to consider a more general consensus dynamics and disagreement with antagonistic behaviour of the agents interacting on a network.

Financial theory literature linked predictability, such as momentum, reversal and spillovers effects to disagreement among investors. For instance, Cujean and Hasler (2017) show that stronger autocorrelation levels in a risky asset is found during bad times when considering two agents with different predicting models. Han et al. (2017) found spillovers (cross-autocorrelation) in two risky assets arises when considering two agents. Serial correlation in the same asset and between different assets signals disagreement. Thus in this paper we consider networks of serial correlation for studying the opinion dynamics on prices. If consensus is reached then serial correlation is reduced.

The paper is structured as follows. Section 2 provides some background on graph theory for network analysis. In Section 3, we introduce the notions of disagreement and consensus dynamics for directed networks. Section 4 extends the results of Section 3 to signed networks. Section 5 provides some empirical results on both simulated and real-world financial networks.

2 Financial Networks and Graph Theory

A network can be defined as a set of vertices (or nodes) and arcs (or edges) between vertices. In financial networks, a node represents a financial institution (e.g., a bank, an insurance company, a financial agglomeration) and an edge has the interpretation of financial linkage between two institutions. In

mathematical terms a network can be represented through the notion of graph and its properties. In the following sections we provide some background in graph theory useful for a better comprehension of the new indicators developed in this paper and of the analysis of financial networks. For further material on graph theory and random graph we refer the interested reader to Bollobás (1998) and Bollobás (2001). See Jackson (2008) for an introduction to network theory in social sciences.

A graph is defined as the ordered pair of sets $G = (V, E)$ where $V = \{1, \ldots, n\}$ is the set of vertices (or nodes) and $E \subset V \times V$ the set of edges (or arcs). The order of a graph is the number of vertices in V, that is the cardinality of V denoted with $|V|$. An (directed) edge between two nodes exists if there is a relationship between them and it can be identified as the (ordered) pair $\{u, v\}$ with $u, v \in V$. If there is no direction in the connection between nodes then an edge $\{u, v\}$ is an unordered pair of nodes and the graph G is said to be undirected, whereas if a direction exists, then each edge $\{u, v\}$ is defined as an ordered pair of nodes and the graph G is said to be directed graph (or digraph).

Assume for simplicity the graph $G = (V, E)$ is undirected. If $\{u, v\} \in E$ then u and v are adjacent vertices and they are incident with the edge $\{u, v\}$. For each node u, it possible to define its neighborhood as the set of nodes adjacent to u, that is $N_u = \{v \in V; \{u, v\} \in E\}$. The vertex adjacency structure of a n-order graph $G = (V, E)$ can be represented through a n-dimensional matrix A called adjacency matrix. Each element a_{uv} of the adjacency matrix is equal to 1 if there is an edge from institution u to institution v with $u, v \in V$, and 0 otherwise, where $u \neq v$, since self-loops are not allowed. If the graph is undirected than $a_{uv} = a_{vu}$, that is the adjacency matrix is symmetric.
As an example, Figure 1 includes two graphs, one directed (panel (a)) and the other undirected (panel (b)). The edges of the directed graph are $e_1 = \{v_2, v_1\}$, $e_2 = \{v_2, v_4\}$, $e_3 = \{v_2, v_3\}$ and $e_4 = \{v_3, v_4\}$ and its adjacency matrix is given in the second line of the same panel. The edges of the undirected graph are $e_1 = \{v_1, v_2\}$, $e_2 = \{v_1, v_4\}$, $e_3 = \{v_3, v_4\}$ and its adjacency matrix is given in the second line of the same panel.

In some applications it is useful to focus the analysis on a subset of nodes or edges of a graph. We say that $G' = (v', E')$ is a subgraph of G if $V' \subset V$ and $E' \subset E$. The subgraph can be induced by a subset of edges or by a subset of nodes. Panel (c) of Figure 1 shows, as an example, the subgraph of the directed

graph reported in Panel (a). Given two subgraphs of G, $G_1 = (V_1, E_1)$ and $G_2 = (V_2, E_2)$, the graph union $G_3 = G_1 \cup G_2$ is defined as the graph $G_3 = (V_3, E_3)$ such that $V_3 = V_1 \cup V_2$ and $E_3 = \{\{u, v\} \in E; u, v \in V_3\}$. Note that $E_1 \cup E_2 \subset E_3$. The graph difference $G_3 = G_2 \backslash G_1$ with $V_1 \subset V_2$, is defined as the graph $G_3 = (V_3, E_3)$ such that $V_3 = V_2 \backslash V_1$ and $E_3 = \{\{u, v\} \in E; u, v \in V_3\}$.

INSERT FIGURE 1 HERE

2.1 Graph Connectivity

Let $G = (V, E)$ be an undirected graph, a simple measure of connectivity is the node degree which is the number of adjacent nodes. If a_{uv} is the u-th row and v-th column element of the adjacency matrix A, then the degree of the node u is

$$d_u = \sum_{v=1}^{n} a_{uv} \tag{1}$$

If $G = (V, E)$ is a directed graphs, it is possible to define the number of edges directed from other nodes to node u (in-degree) and from node u to other nodes (out-degree)

$$d_u^{out} = \sum_{v=1}^{n} a_{vu}, \quad d_u^{in} = \sum_{v=1}^{n} a_{uv} \tag{2}$$

The two extreme configurations of the connectivity structure of a n-order graph G are given by the graph with empty edge set, i.e. $|E| = 0$, which is called empty graph and denoted with E_n and the complete graph where each node is adjacent to all other nodes in the graph. In this case, the cardinality of the edge set is maximal, i.e. $|E| = n(n-1)/2$, and graph is denoted with K_n. Panels (a) and (b) of Figure 2 show an example of complete, K_4, and empty, E_4, graphs. The number of elements in the edge set is called volume of G, that is $\mathrm{vol}(G) = |E|$.

The node degree measures rely on the adjacency of the nodes and do not account for cohesiveness and indirect connectivity patterns which play a crucial role in spreading of contagion in a network. The cohesiveness can be represented through the number and size of cliques or of communities, and the indirect connections can be represented by walks, trails, paths, circuits and cycles.

A clique $C \subset G$, is defined as an ordered pair of sets $C = (V_C, E_C)$ with

5

$V_C \subset V$ and $E_C = \{\{u, v\} \in E; u, v \in V_C\}$ such that $m = |V_C| > 2$, $E_C = K_m$ and $C \cup \{w\}$ with $w \in G \backslash C$ is not complete.

A walk $W_{uv} = (v_0, e_1, \ldots, e_l, v_l)$ between two vertices u and v of G, called endvertices, is identified by an alternating sequence of (not necessary distinct) vertices $V(W_{uv}) = \{v_0, v_1, \ldots, v_l\}$ and edges $E(W_{uv}) = \{e_1, \ldots, e_l\} \subset E$, with $e_1 = (v_0, v_1)$, $e_l = \{v_{l-1}, v_l\}$, and $v_0 = u$ and $v_l = v$. The number of edges $|E(W_{uv})| = l$ in a walk is called "walk length". A walk of length l is called l-walk and denoted with W_l. It is easy to show that the number of l-walks from node u to node v is equal to the (u, v)-th element of A^l that is equal to

$$\sum_{v_1=1}^{n} \sum_{v_2=1}^{n} \cdots \sum_{v_{l-1}=1}^{n} a_{uv_1} a_{v_2 v_3} \ldots a_{v_{l-1} v}. \tag{3}$$

If all edges are distinct then the walk is called a trail. A trail with coincident endvertices is called a circuit (or closed trail). A walk W_l with $l \geq 3$ with $v_0 = v_l$ and vertices v_j, $0 < j < l$ distinct from each other and from v_0, is called cycle and denoted with C_l. An example of cycle C_4 is given in panel (d) of Figure 2.

A path P_{uv} between vertices u and v of G is a walk with distinct elements in its vertex set. A generic path of length l is denoted with l. The shortest-path P_{uv}^* between two vertices u and v is $\min_{l}\{P_{uv} = (v_0, e_1, \ldots, e_l, v_l), l \geq 1\}$ that is the path with the minimum length. An example of path P_2 is given in panel (c) of Figure 2.

The notion of path allows us to introduce the definition of connected graph and some other basic graph structures. A graph is connected if for every pair of distinct vertices u and v there is a path from u to v. A maximal connected subgraph is a component of the graph. A cutvertex is a vertex whose deletion increases the number of components. An edge is a bridge if its deletion increases the number of components. A graph without cycles is a forest or an acyclic graph. A tree is a connected forest.

INSERT FIGURE 2 HERE

The notion of path can be used to define the distance between two nodes u and v, $d(u, v)$ as the length of the shortest path or geodesic between u and v. See Billio et al. (2019a) for further background material on graph theory for financial network analysis.

Another notion which is relevant to the results discussed in this paper is the one of random walk on a graph. Let $G = (V, E)$ be a connected graph with vertex set $V = \{1, 2, \ldots, n\}$. A sequence of random vertices $\{v_t\}_{t \geq 0}$ with $v_t \in V$ is a random walk on G starting at the node v_0 if at the $(t+1)$-th step the random variable v_{t+1} takes value i with probability $1/d_{v_t}$ where i belongs to the neighbour N_{v_t}. If we define

$$p_{ij} = \begin{cases} 1/d_i & \{i, j\} \in E \\ 0 & \{i, j\} \notin E \end{cases}$$

then $M = (p_{ij})_{i,j \in V}$ is a matrix of transition probabilities and the sequence $\{v_t\}_{t \geq 0}$ is a Markov chain process. The transition matrix can be written as $M = D^{-1}A$ where $D = \text{diag}\{d_1, \ldots, d_n\}$ is a diagonal matrix and A the adjacency matrix of G. If the graph G is connected and not bipartite the random walk converges to the stationary distribution of M, $\boldsymbol{\pi} = (\pi_1, \ldots, \pi_n)$ with $\pi_i = d_i/(2\text{vol}(G))$ which satisfies

$$M' \boldsymbol{\pi} = A D^{-1} (d_1, \ldots, d_n)' \frac{1}{2\text{vol}(G)} = \left(\sum_{i=1}^{n} a_{1i} \frac{d_i}{d_i}, \ldots, \sum_{i=1}^{n} a_{ni} \frac{d_i}{d_i} \right) \frac{1}{2\text{vol}(G)} = \boldsymbol{\pi}. \tag{4}$$

The stationary distribution and the spectrum of $D^{1/2} M D^{-1/2}$ are connected by the following equation

$$M^t = \boldsymbol{\pi} \boldsymbol{\pi}' + \sum_{k=2}^{n} \lambda_k^t D^{-1/2} \mathbf{v}_k \mathbf{v}_k' D^{1/2} \tag{5}$$

where $1 = \lambda_1 \geq \lambda_2 \geq \ldots \geq \lambda_n > -1$ and $\mathbf{v}_1, \ldots, \mathbf{v}_n$ satisfies the spectral representation

$$D^{1/2} M D^{-1/2} = \sum_{k=1}^{n} \lambda_k \mathbf{v}_k \mathbf{v}_k' \tag{6}$$

In the study of opinion dynamics another type of random walk process is used: the lazy random walk. This process is a random walk with transition matrix $P_L = (I + D^{-1}A)/2$. If G is connected the lazy walk converges to the stationary distribution $\pi(v) = d_v/\text{vol}(G)$. We refer the reader to Lovász (1996) for a review on random walks on a graph.

3 Disagreement and Networks

The relationship between the eigenvalues of the directed Laplacian (Diplacian), introduced in Li and Zhang (2012), and the rate of convergence to a consensus of agents interacting on a network was studied in Billio et al. (2018). The application of those techniques to financial networks could be understood as measuring persistence of disagreement that is "magnified when major events occur in financial markets" according to Carlin et al. (2014). Our approach considers a limited communication network Parikh and Krasucki (1990) among agents, represented by statistical causal relationships between stock returns as done in Billio et al. (2018).

Consider a graph with adjacency matrix $A = (a_{ij})_{ij}$ with non-negative elements, $a_{i,j} \in \mathbb{R}_+$, and the diagonal matrix D with non zero elements $d_i^{out} = \sum_{j=1}^{n} a_{ij}$ $i = 1, \ldots, n$ on the main diagonal. In our model for disagreement persistence (or opinion dynamics on network), we assume the variable $x_{i,t} \in \mathbb{R}$ represents the opinion of an agent $i \in \{1, \ldots, n\}$ at time t and the coefficient a_{ij} the interaction effect between two agents i and j. Also, we introduce the following discrete time dynamic system describing the interaction between the agents:

$$x_{it} = x_{it-1} + \frac{1}{2d_i^{out}} \sum_{j=1}^{n} a_{ij} \left(x_{jt-1} - x_{it-1} \right) \tag{7}$$

Since $a_{ij} \geq 0$ the opinion of the agent i is attracted by the opinion of the agent j. Similar systems, introduced by DeGroot (1974), are building blocks in models for belief evolution of agents with bounded rationality and with a persuasion bias DeMarzo et al. (2003).

The model can be written in the matrix form:

$$\mathbf{x}_t = \left(\frac{1}{2}I_n + \frac{1}{2} \left(I_n - D^{-1} \left(D - A \right) \right) \right) \mathbf{x}_{t-1} = P_L \mathbf{x}_{t-1}$$

Where $\mathbf{x}_t = (x_{it}, \ldots, x_{nt})$ is the state vector of the agents and $P_L = (I_n - P)$, with $P = D^{-1}A$, is the transition matrix of a lazy random walk (Chung, 2005). The matrix $P = D^{-1}A$ is the transition probability matrix of the Markov chain associated with random walks on G, where the (i, j)–th element of P is

$$p_{ij} = \begin{cases} \frac{1}{d_i^{out}} a_{ij} & \text{if } \{i, j\} \in E \\ 0 & \text{otherwise.} \end{cases}$$

and represent the probability of transitioning from vertex i to vertex j of a random walk starting at i. If the graph is strongly connected, P_L is irreducible and aperiodic, according well known results, the system converge to a consensus with group decision value $\varphi'\mathbf{x}_0$. The group decision is conserved by the dynamics:

$$\varphi'\mathbf{x}_t = \varphi'P_L\mathbf{x}_{t-1}\varphi'\mathbf{x}_{t-1} = \alpha.$$

We define the disagreement vector $\boldsymbol{\xi}_t$ as follows

$$\boldsymbol{\xi}_t = \mathbf{x}_t - \alpha\mathbf{1}$$

and its law of motion

$$\boldsymbol{\xi}_t = P_L\boldsymbol{\xi}_{t-1}.$$

The disagreement dynamics allows us to study the convergence rate in this directed unsigned case to this decision value. We exploit the theoretical results on lazy random walks on strongly connected directed graphs due to Chung (2005) and Li and Zhang (2012). In particular in Li and Zhang (2012) the Diplacian Γ and its decomposition of in symmetric and asymmetric part is introduced

$$\Gamma = \varphi^{1/2}\left(I - P\right)\varphi^{-1/2}, \quad \Gamma = L + \Delta, \quad L = \frac{\Gamma + \Gamma'}{2}, \quad \Delta = \frac{\Gamma - \Gamma'}{2}.$$

where $\varphi = \mathrm{diag}(\boldsymbol{\varphi})$ is a diagonal matrix and $\boldsymbol{\varphi}$ the ergodic probability vector of the Markov chain with transition matrix P^2. According to the results in Billio et al. (2019a) the speed of convergence to the consensus can be written as a function of the second smallest eigenvalue of L, λ_2, the second largest singular value of $I_n - L$, $\sigma_{n-1}\left(I_n - L\right)$, and the largest singular value of the skew-symmetric part of the diplacian Δ, $\sigma_n\left(\Delta\right)$, as stated in the following theorem.

Theorem 1. Consider the discrete-time system introduced in (5) on a a strongly connected directed network. A consensus is globally exponentially

reached according to

$$
\begin{aligned}
\|\xi_t\| &\leq \exp\left\{\frac{1}{2}\left[\log\left(\frac{\max(\boldsymbol{\varphi})}{\min(\boldsymbol{\varphi})}\right)+\log(\mu)\,t\right]\right\}\|\xi_0\| \\
\mu &= \frac{3}{4}-\frac{\lambda_2}{2}+\frac{(\sigma_{n-1}(I_n-\Gamma))}{4} < \frac{3}{4}-\frac{\lambda_2}{2}+\frac{(\sigma_{n-1}(I_n-L)+\sigma_n(\Delta))^2}{4}.
\end{aligned}
$$

where μ is the disagreement persistence index, measuring the convergence rate to consensus

See Billio et al. (2019a) for a proof. The result in Theorem 1 implies a slower convergence if the graph is directed and shows a magnifying effect of the heterogeneity in the importance of the nodes in the common decision of the group.

4   Disagreement and Signed Networks

In the previous section the elements of the adjacency matrix, a_{ij}, were assumed to be non-negative. In many applications, networks are extracted by vector autoregressions (VAR), or similar methodologies, which allow for weighted networks with possibly negative edge weights. Usually, the network topology is analysed considering the absolute value of the edge weights. As argued in various papers (see, e.g. Altafini, 2012, 2013), neglecting the signs of the weights can lead to wrong conclusions on the connectivity structure and produce a relevant loss of information about the contagion dynamics.

Consider a signed network that is an adjacency matrix A with real-valued elements, $a_{ij}\in\mathbb{R}$, $i,j=1,\ldots,n$. A signed framework to network analysis consists in studying the antagonistic interaction among agents, i.e.

$$
x_{it} = x_{it-1}+\frac{1}{2d_i^{|out|}}\sum_{j=1}^{n}|a_{ij}|\left(\operatorname{sign}(a_{ij})\,x_{jt-1}-x_{it-1}\right). \tag{8}
$$

Since a_{ij} can be either positive or negative, in the system there two types of effects. If $a_{ij}\geq 0$ the opinion of the agent i is attracted by the opinion of the agent j, whereas if $a_{ij}\leq 0$ the opinion of the agent i is attracted by the opinion opposite to that of agent j. As argued in Hendrickx (2014), this model allows not only for convergence of opinions toward a common value but also for persistent disagreement and multiple clusters of opinions. The behaviour of the system depends crucially on the topology of the network and on the

signs of the edge weights a_{ij}. The following examples illustrate the roles of signs in reaching the consensus. In the first example (top plots of Fig. 3) we let $x_0 = (0.5, 0)$ be the initial value of the agent opinions and

$$A = \begin{pmatrix} 0 & -1/4 \\ -1/4 & 0 \end{pmatrix}$$

be the adjacency matrix. In the second example (bottom plots of Fig. 3) we assume the initial value of the agent opinions are randomly selected as follows $x_0 = (u_1 v_1, \ldots, u_{100} v_{100})$, with u_i and v_i standard uniform and Bernoulli variables, respectively. The edge weights are $a_{ij} = (i - j)/100$.

In both settings, we consider the opinion dynamics in the classical consensus system assuming alternatively a_{ij} and $|a_{ij}|$ as interaction coefficients. In the first case the two agents reach consensus as $t \to \infty$ (left plots in Fig. 3) whereas in the second case the agents opinions diverge (right plots).

<div align="center">INSERT FIGURE 3 HERE</div>

The antagonistic interaction in Equation 8 can be written as a classical consensus system, with unsigned directed interactions, by applying the clever lifting trick introduced in Hendrickx (2014). Let us define $b_{ij} = \max(0, a_{ij})$, $c_{ij} = \max(0, -a_{ij})$, $d_i^{|out|} = \sum_{j=1}^{n} |a_{ij}|$ then the dynamic in Eq. 8 can be written as

$$x_{it} - x_{it-1} = \frac{1}{2d_i^{|out|}} \sum_{j=1}^{n} b_{ij} (x_{jt-1} - x_{it-1}) - \frac{1}{2d_i^{|out|}} \sum_{j=1}^{n} c_{ij} (x_{jt-1} + x_{it-1}) \quad (9)$$

and

$$y_{it} - y_{it-1} = \frac{1}{2d_i^{|out|}} \sum_{j=1}^{n} c_{ij} (y_{jt-1} - y_{it-1}) - \frac{1}{2d_i^{|out|}} \sum_{j=1}^{n} b_{ij} (y_{jt-1} + y_{it-1}) \quad (10)$$

where the two systems are coupled by the relationship $y_{it} = -x_{it}$. The joint dynamics can be written

$$\begin{bmatrix} \mathbf{x}_t \\ \mathbf{y}_t \end{bmatrix} = \left(\frac{1}{2} \begin{bmatrix} I_n & \mathbf{0} \\ \mathbf{0} & I_n \end{bmatrix} - \frac{1}{2} \begin{bmatrix} (D^{|out|})^{-1} & \mathbf{0} \\ \mathbf{0} & (D^{|out|})^{-1} \end{bmatrix} \begin{bmatrix} B & C \\ C & B \end{bmatrix} \right) \begin{bmatrix} \mathbf{x}_{t-1} \\ \mathbf{y}_{t-1} \end{bmatrix} \quad (11)$$

where

$$B = \begin{pmatrix} b_{11} & \cdots & b_{1n} \\ \vdots & & \vdots \\ b_{n1} & \cdots & b_{nn} \end{pmatrix}, C = \begin{pmatrix} c_{11} & \cdots & c_{1n} \\ \vdots & & \vdots \\ c_{n1} & \cdots & c_{nn} \end{pmatrix},$$

$$D^{|out|} = \begin{pmatrix} d_1^{|out|} & 0 & \cdots & 0 \\ 0 & d_2^{|out|} & \cdots & 0 \\ \vdots & \vdots & \ddots & \vdots \\ 0 & 0 & \cdots & d_n^{|out|} \end{pmatrix}$$

Analogously to Hendrickx (2014) $\mathbf{x}_t$ is a solution of (11) if and only if $\mathbf{z}_t = (\mathbf{x}_t, \mathbf{y}_t)$ is a solution of the "classical" discrete time consensus system

$$\begin{bmatrix} \mathbf{x}_t \\ \mathbf{y}_t \end{bmatrix} = P_L \begin{bmatrix} \mathbf{x}_{t-1} \\ \mathbf{y}_{t-1} \end{bmatrix}$$

where the lifted transition probability is

$$P_L = \frac{1}{2} \begin{bmatrix} I_n & \mathbf{0} \\ \mathbf{0} & I_n \end{bmatrix} - \frac{1}{2} \begin{bmatrix} \left(D^{|out|}\right)^{-1} & \mathbf{0} \\ \mathbf{0} & \left(D^{|out|}\right)^{-1} \end{bmatrix} \begin{bmatrix} B & C \\ C & B \end{bmatrix}. \tag{12}$$

The decision vector and Laplacian corresponding to P_L can be used in Theorem 1 to bound the speed of convergence of the lifted dynamics and to find an upper bound for consensus dynamics on a signed directed network. As discussed for the unsigned case in Billio et al. (2018), those results can be readily applied to build a disagreement index which includes the sign information. A comparison with the unsigned framework can provide a better understanding of the roles of the negative weights in financial connectedness and systemic risk. In this paper, we apply the following two disagreements measures:

- the disagreement persistence

$$\mu = \frac{3}{4} - \frac{\lambda_2}{2} + \frac{(\sigma_{n-1}(I_n - \Gamma))}{4}$$

  which measures the fraction of disagreement present in the system after one period;

- the half life of disagreement

$$\tau_{1/2\xi} = -\frac{\log\left(\dfrac{\max(\boldsymbol{\varphi})}{\min(\boldsymbol{\varphi})}\right)}{\log(\mu)}$$

which indicates the time the disagreement vector norm takes to reduce by one half.

5 Empirical Analysis

In this section we provide some empirical applications to synthetic and real data. Network analysis proved to be an efficient methodology to measure connectedness in financial systems. Scholars have introduced several inference approaches on financial networks. In this paper, we consider a rolling window parametric estimates of the connectedness following two of most compelling approaches.

The first one is due to Billio et al. (2012) which proposes to extract connectedness between stock returns by pairwise Granger causality tests, that is by estimating

$$r_{it} = \phi_{ii} r_{it-1} + \phi_{ij} r_{jt-1} + \varepsilon_{it}$$

and by setting

$$A_{GC,ij} = \begin{cases} 1 & \text{if } \phi_{ij} \text{ statistically different from } 0 \\ 0 & \text{otherwise} \end{cases}$$

where $r_{i,t} = \log(P_{i,t}) - \log(P_{i,t-1})$ $i = 1, \ldots, n$ are logarithmic returns on n assets.

The second approach proposed by Diebold and Yılmaz (2014) applies the H-step generalized variance decomposition of a VAR model. Assume a VAR model of the first order

$$\mathbf{r}_t = \Phi \mathbf{r}_{t-1} + \boldsymbol{\varepsilon}_t, \ \boldsymbol{\varepsilon}_t \overset{iid}{\sim} N(\mathbf{0}, \Sigma) \tag{13}$$

where $\mathbf{r}'_t = (r_{1,t}, \ldots, r_{n,t})$. The estimated autoregressive coefficients $\hat{\Phi}$ and covariance matrix $\hat{\Sigma}$ are used to compute the connectedness matrices $\hat{D}_h$, $h =$

$1, \ldots, H$ with elements

$$\hat{D}_{h,ij} = \frac{\hat{\sigma}_{jj}^{-2} \sum\limits_{\ell=0}^{h-1} \left(\left[\left(\hat{\Phi} \right)^{\ell} \sqrt{\hat{\Sigma}} \sqrt{\hat{\Sigma}}^{T} \right]_{ij} \right)^2}{\sum\limits_{\ell=0}^{h-1} \left[\left(\hat{\Phi} \right)^{\ell} \sqrt{\hat{\Sigma}} \sqrt{\hat{\Sigma}}^{T} \left(\hat{\Phi}^{T} \right)^{\ell} \right]_{ij}}, \; i,j = 1, \ldots, n$$

and the corresponding weight matrix $A_D = \hat{D}_h - \text{diag}\left(\hat{D}_h \right)$ of a signed and directed weighted network (Diebold and Yılmaz (2014)). Alternatively, we use $\hat{\Phi}$ to compute the forecast operator $\hat{\Phi}_h = \sum_{\ell=0}^{h} (\hat{\Phi})^{\ell}$ and the weight matrix $A_{\Phi} = \hat{\Phi}_h - \text{diag}\left(\hat{\Phi}_h \right)$ of a signed directed weighted network.

In the following applications, we study the autoregressive coefficients $\hat{\Phi}$, the global connectedness

$$C_h = \frac{1}{n} \sum_{\substack{i,j=1 \\ i \neq j}}^{n} \hat{A}_{D,ij}$$

and the disagreement persistence measures, $\mu\left(A_D \right)$ and $\mu\left(A_{\Phi} \right)$, and the half life of disagreement $\tau_{\xi/2}\left(A_D \right)$ and $\tau_{\xi/2}\left(A_{\Phi} \right)$.

5.1 Simulated Networks

Following the prediction from the financial theory (e.g., see Chan (1993)) asymmetric information, disagreement and predictability are strictly related. Assume the stocks are traded over T periods and the stock log-value is given by

$$V_{i,t} = \bar{v} + \sum_{\tau=1}^{t} \Delta V_{i,\tau} \tag{14}$$

$$\Delta V_{i,t} = M_t + \epsilon_{i,t} \tag{15}$$

where $\Delta V_{i,t}$ represents the change in the stock log-value, $\epsilon_{i,t}$ is a stock-specific information component that affects stock i at time t and M_t a market-wide information component that affects all stocks. We assume that the market factor and the stock idiosyncratic terms are independent that is

$$(M_t, \epsilon_t)' \overset{iid}{\sim} N\left(\mathbf{0}_2, \text{diag}\left(\sigma_M^2, \sigma_\epsilon^2 \right) \right)$$

14

Assume there is one market maker for each stock i which observes directly the true increment of the log-value $\Delta V_{i,\tau}$, $\tau = 1, \ldots, t - 1$, does not observe directly the current increment $\Delta V_{i,t}$ but instead observes the signal $\theta_{i,t}$ where

$$\theta_{i,t} \;=\; \Delta V_{i,t} + \eta_{i,t} \tag{16}$$

where $\eta_{i,t} \sim N(0, \sigma_\eta^2)$ and $Cov(\eta_{i,t}, \eta_{j,s}) = Cov(\eta_{i,t}, M_s) = 0$ for all $i \neq j$ and $s, t = 1, \ldots, T$. Conditionally on his information set, the market maker i sets the log-price as

$$\log P_{i,t} \;=\; \bar{v} + \sum_{\tau=1}^{t-1} \Delta V_{i,\tau} + \kappa \theta_{i,t} \tag{17}$$

where

$$\kappa = \frac{\sigma_M^2 + \sigma_\epsilon^2}{\sigma_M^2 + \sigma_\epsilon^2 + \sigma_\eta^2}$$

It can be shown (see Chan (1993)) that the cross-autocorrelation generated by the disagreement is

$$\mathrm{Corr}\left(\Delta \log P_{i,t}, \Delta \log P_{j,t-1}\right) \;=\; \kappa\left(1 - \kappa\right) \frac{\sigma_M^2}{\sigma_M^2 + \sigma_\epsilon^2}$$

Figure 4 provides a numerical illustration of the auto cross-correlation level for different levels of disagreement (horizontal axis) and market volatility (different lines).

<div align="center">INSERT FIGURE 4 HERE</div>

In empirical applications, the disagreement level ($\sigma_\eta^2 > 0$) and the serial cross-correlation are not observable, but can be inferred from observed data. We generate $T = 12000$ samples from the model given above with the following parameters setting: $\bar{v} = 1000$, $\sigma_M^2 = 1$, $\sigma_\epsilon^2 = 0.1$, $\sigma_\eta^2 = 0.1$ if $t < 6000$ and $\sigma_\eta^2 = 0.7$ if $t \geq 6000$. Figure 5 shows the $N = 40$ simulated series of asset prices. For the simulated data, we consider a sequence of 100 not overlapping windows of 120 observations each, and estimate for each window the autocorrelation matrix (see Figure 6), the autoregressive coefficients matrix, its spectral radius and its total degree, see the shaded blue area(left axis), the solid line and the dashed line (right axis) in Figure 7). Figure 8 shows the disagreement

<div align="center">15</div>

persistence $\tau_{\xi/2}(A_D)$ (blue line, left axis), and half-life disagreement $\mu(A_D)$ (red line, right axis).

INSERT FIGURES 5 - 8 HERE

5.2 Stock Market Networks

In the empirical analysis, we consider the financial connectedness in the European area. The dataset is composed of daily returns for value-weighted financial institutions stock indexes for 19 European countries from 8th January 1996 to 30th December 2016.[1] Data have been downloaded from Eikon/Datastream.

Following Billio et al. (2012), we estimate dynamic Granger networks using rolling windows with length size of 252 daily observations, that is approximately one year. We estimate in each window a VAR(1) using a penalized regression approach with an Elastic Net penalty to obtain the spillover index D_h and Φ_h with an horizon h form 1 to 12 days. The tuning parameter is chosen by cross-validation using the *sparsevar* R package[2].

We compute connectedness, half life of disagreement and disagreement persistence on D_h and half life of disagreement and disagreement persistence on Φ_h.

We study if our measures are statistically related to other measures of disagreement, such as the Economic Sentiment Indicator (ESI) of the European Commission[3]. ESI is based on regular harmonized surveys, conducted by the Directorate General for Economic and Financial Affairs for different sectors of the economies in the European Union (EU) and in the applicant countries It is a composite indicator on five weighted sectoral confidence indicators: Industrial confidence indicator, Services confidence indicator, Consumer confidence indicator, Construction confidence indicator, and Retail trade confidence indicator. In this respect, we consider the monthly sentiment indicators for the 19 European Economies included in our dataset and compute their cross-sectional standard deviation $(\hat{\sigma}_{ESI})$ at each point in time. Is worth noting that the obtained measure $\hat{\sigma}_{ESI}$ describes disagreement about the condition of the

---

[1]The countries considered are Austria, Belgium, Czech Republic, Denmark, Finland, France, Germany, Greece, Hungary, Ireland, Italy, Netherlands, Norway, Poland, Portugal, Spain, Sweden, Switzerland and the United Kingdom.

[2]The Package is available at https://cran.r-project.org/web/packages/sparsevar/sparsevar.pdf.

[3]The ESI indicator is available at https://data.europa.eu/euodp/it/data/dataset/cO4BuUz6WXIQGJkHPwLug

whole European economic system and not just the financial system. Therefore, the higher the cross-sectional standard deviation, the higher the disagreement about the economic condition between the European Countries.

<div align="center">INSERT FIGURE 9 HERE</div>

To compare the proposed measures with the ESI indicator, we sample the estimated $\hat{\Phi}$ in each window which corresponds to the last day of the month and perform a regression analysis. Figure 9 shows the total connectedness C_h and the cross-sectional standard deviation of national ESI indicators, $\hat{\sigma}_{ESI}$. As expected, the total connectedness increases during turbulent market periods while the cross-sectional deviation of ESI indicators picks up after the Asian crisis in 1997-98 and after global financial crisis in 2007-2008.

<div align="center">INSERT FIGURES 10-11 HERE</div>

Figure 10 includes on the left-scale the half life of disagreement on connectedness ($\tau_{\xi/2}(A_D)$) and the half life disagreement on the forecast operator ($\tau_{\xi/2}(A_\Phi)$) while on the right-scale the cross-sectional standard deviation of national ESI indicators($\hat{\sigma}_{ESI}$).

Figure 11 shows the disagreement persistence on connectedness ($\mu(A_D)$), the disagreement persistence on the forecast operator ($\mu(A_\Phi)$) and the cross-sectional standard deviation of national ESI indicators($\hat{\sigma}_{ESI}$).

Table 1 shows the estimated models where the dependent variable is the cross-sectional standard deviation of national ESI indicators $\hat{\sigma}_{ESI}$ and the explanatory variables are the total connectedness C_h, the half life of disagreement on connectedness $\tau_{\xi/2}(A_D)$, the half life disagreement on the forecast operator $\tau_{\xi/2}(A_\Phi)$, the disagreement persistence on connectedness $\mu(A_D)$ and the disagreement persistence on the forecast operator $\mu(A_\Phi)$. First, the total connectedness (C_h) and the half life disagreement on the forecast operator $\tau_{\xi/2}(A_\Phi$ are not significantly different from zero both at 1% and 5% confidence level while the half life of disagreement on connectedness $\tau_{\xi/2}(A_D)$ is significantly different from zero at 5% with an estimated coefficient equal to 0.0160. Both the disagreement persistence on connectedness $\mu(A_D)$ and the disagreement persistence on the forecast operator $\mu(A_\Phi)$ are significantly different from zero at 1% confidence level with estimated coefficients equal to 0.8169 and 0.6529, respectively. In all cases, the coefficients are positive indicating a positive relationship among disagreement in the financial network and the cross-sectional standard deviation of national ESI indicators($\hat{\sigma}_{ESI}$).

<div align="center">17</div>

INSERT TABLE 1 HERE

6 Conclusion

Networks extraction from financial time series relies on different techniques (e.g., Granger causality, Sims causality, sparse VAR, graphical VAR). Building on financial theoretic literature, we study consensus dynamics on financial weighted networks and propose two new measures: time to consensus and disagreement persistence. Our results extend the existing consensus dynamic to weighted directed networks, with signed weighting matrix. We provide an empirical investigation of the adequateness of the proposed measures and a comparison with a financial disagreement proxy. Our findings suggest that the new measures outperform the simple total connectedness measure, and are able to capture different characteristics of the data that better resemble disagreement. Our disagreement proxy is based on a country aggregated sentiment index about economic expectation of which financial are only a part, this could explain the small explanatory power of our regression analysis.

References

D. F. Ahelegbey, M. Billio, and R. Casarin. Sparse graphical multivariate autoregression: A Bayesian approach. *Annals of Economics and Statistics*, 123/124:1–30, 2016a.

D. F. Ahelegbey, M. Billio, and R. Casarin. Bayesian graphical models for structural vector autoregressive processes. *Journal of Applied Econometrics*, 2(31):357–386, 2016b.

C. Altafini. Dynamics of opinion forming in structurally balanced social networks. *Plos One*, 7(6):1–9, 2012.

C. Altafini. Consensus problems on networks with antagonistic interactions. *IEEE Transactions on Automatic Control*, 58(4):935–946, 2013.

D. Bianchi, M. Billio, R. Casarin, and M. Guidolin. Modeling systemic risk with Markov switching graphical SUR models. *Journal of Econometrics*, 210(1):58–74, 2019.

M. Billio, M. Getmansky, A. W. Lo, and L. Pelizzon. Econometric measures of connectedness and systemic risk in the finance and insurance sectors. *Journal of Financial Economics*, 104(3):535–559, 2012.

M. Billio, R. Casarin, M. Costola, and L. Frattarolo. Disagreement in signed financial networks. In *Mathematical and Statistical Methods for Actuarial Sciences and Finance, Corazza, M., Durbán, M., Grané, A., Perna, C., Sibillo, M. (eds.)*. Springer, 2018.

M. Billio, R. Casarin, M. Costola, and L. Frattarolo. Contagion dynamics on financial networks. In *International Financial Markets, Chevallier, J., Goutte, S., Guerreiro, D., Saglio, S. and Sanhaji, B. (eds)*, volume 1. Routledge, 2019a.

M. Billio, R. Casarin, and L. Rossini. Bayesian nonparametric sparse VAR models. *Journal of Econometrics*, 212(1):97–115, 2019b.

B. Bollobás. *Modern Graph Theory*. Springer, 1998.

B. Bollobás. *Random Graphs*. Cambridge University Press, 2001.

B. I. Carlin, F. A. Longstaff, and Kyle Matoba. Disagreement and asset prices. *Journal of Financial Economics*, 114(2):226 – 238, 2014.

K. Chan. Imperfect information and cross-autocorrelation among stock prices. *The Journal of Finance*, 48(4):1211–1230, 1993.

F. Chung. Laplacians and the cheeger inequality for directed graphs. *Annals of Combinatorics*, 9(1):1–19, 2005.

J. Cujean and M. Hasler. Why does return predictability concentrate in bad times? *The Journal of Finance*, 72(6):2717–2758, 2017.

M. H. DeGroot. Reaching a consensus. *Journal of the American Statistical Association*, 69(345):118–121, 1974.

P. M. DeMarzo, D. Vayanos, and J. Zwiebel. Persuasion bias, social influence, and unidimensional opinions. *The Quarterly Journal of Economics*, 118(3): 909–968, 2003.

F. X. Diebold and K. Yılmaz. On the network topology of variance decompositions: Measuring the connectedness of financial firms. *Journal of Econometrics*, 182(1):119–134, 2014.

F. X. Diebold and K. Yilmaz. *Financial and Macroeconomic Connectedness: A Network Approach to Measurement and Monitoring.* Oxford University Press, USA, 2015.

B. Han, L. Lu, and Y. Zhou. Two trees with heterogeneous beliefs: Spillover effect of disagreement. *Journal of Financial and Quantitative Analysis*, 2017.

J. M. Hendrickx. A lifting approach to models of opinion dynamics with antagonisms. In *Decision and Control (CDC), 2014 IEEE 53rd Annual Conference on on Decision and Control*, pages 2118–2123. IEEE, 2014.

M. O. Jackson. *Social and Economic Networks.* Princeton University Press, 2008.

Y. Li and Z.-L. Zhang. Digraph laplacian and the degree of asymmetry. *Internet Math.*, 8(4):381–401, 2012.

L. Lovász. Random walks on graphs: A survey. In *Combinatorics Paul Erdos is Eighty, Milos, D. , Sos, V. T., and Szony, T. (eds)*, pages 353–398. János Bolyai Math. Soc., Budapest, Hungary, 1996.

R. Parikh and P. Krasucki. Communication, consensus, and knowledge. *Journal of Economic Theory*, 52(1):178–189, 1990.

	Economic Sentiment Index St. Dev. $\hat{\sigma}_{ESI}$				
(constant)	5.8976***	5.8334***	5.9352***	5.7895***	5.7982***
	(0.0895)	(0.0952)	(0.0890)	(0.0976)	(0.0981)
C_h	0.1890				
	(0.1349)				
$\tau_{\xi/2}(A_D)$		0.0160**			
		(0.0069)			
$\tau_{\xi/2}(A_\Phi)$			0.0002		
			(0.0028)		
$\mu(A_D)$				0.8169***	
				(0.2775)	
$\mu(A_\Phi)$					0.6529***
					(0.2388)
R^2	0.0082	0.0225	0.0000	0.0351	0.0304
Adj-R^2	0.0040	0.0184	-0.0042	0.0311	0.0264
AIC	815.05	811.55	817.02	808.44	809.60
BIC	822.01	818.52	823.98	808.49	816.56
LL	-405.53	-403.78	-406.51	-402.22	-402.80

Table 1: Model specification where the dependent variable is the cross-sectional standard deviation of national ESI indicators ($\hat{\sigma}_{ESI}$) and the explanatory variables are the total connectedness (C_h), the half life of disagreement on connectedness ($\tau_{\xi/2}(A_D)$), the half life disagreement on the forecast operator ($\tau_{\xi/2}(A_\Phi)$, the disagreement persistence on connectedness ($\mu(A_D)$) and the disagreement persistence on the forecast operator ($\mu(A_\Phi)$)). Significance level: 1% (***) and 5% (**). Standard errors in parentheses.
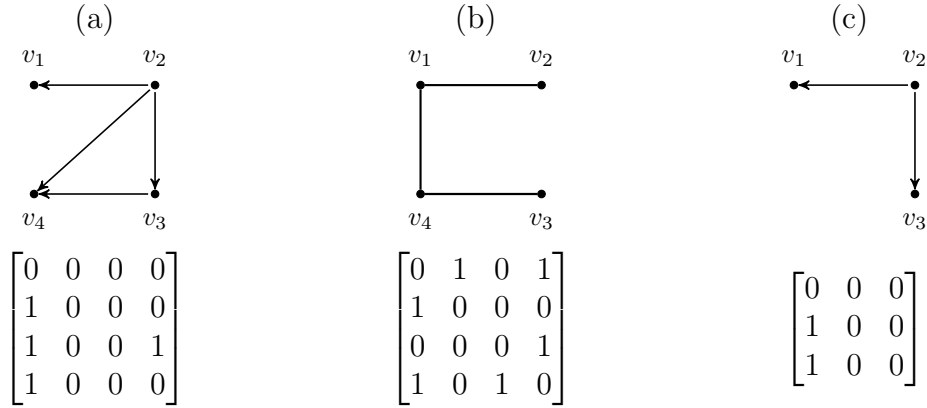
Figure 1: Panel (a): directed graph $G = (V, E)$ (top) with vertex set $V = \{v_1, v_2, v_3, v_4\}$ and edge set $E = \{e_1, e_2, e_3, e_4\}$, where $e_1 = \{v_2, v_1\}$, $e_2 = \{v_2, v_3\}$, $e_3 = \{v_2, v_4\}$, $e_4 = \{v_3, v_4\}$ and its adjacency matrix (bottom). Panel (b): undirected graph $G = (V, E)$ (top) with vertex set $V = \{v_1, v_2, v_3, v_4\}$ and edge set $E = \{e_1, e_2, e_3\}$, where $e_1 = \{v_1, v_2\}$, $e_2 = \{v_1, v_4\}$, $e_3 = \{v_3, v_4\}$ and its adjacency matrix (bottom). Panel (c): subgraph of the graph given in panel (a).
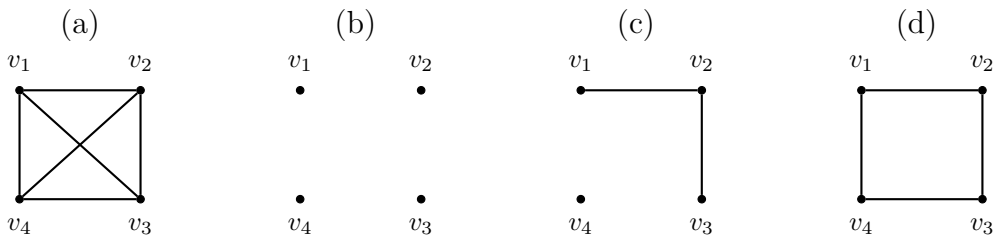
Figure 2: Example of complete graph K_4 (a), empty graph E_4 (b), path P_2 (c) and cycle C_4 (d).
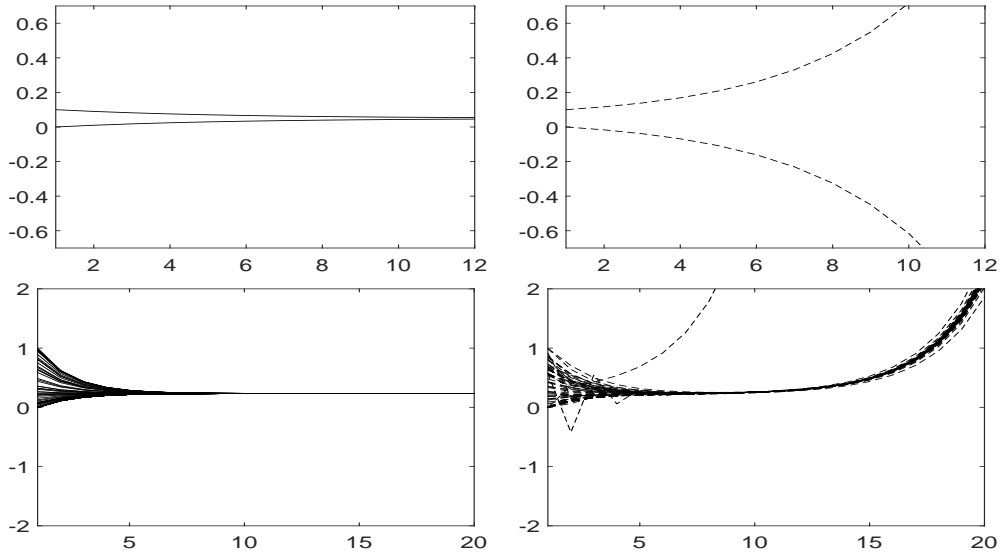
Figure 3: Opinion dynamics over time (horizontal axis) for a system of $n = 2$ (top) and $n = 100$ (bottom) agents interacting on an signed network (left) and on the associated unsigned network (right).
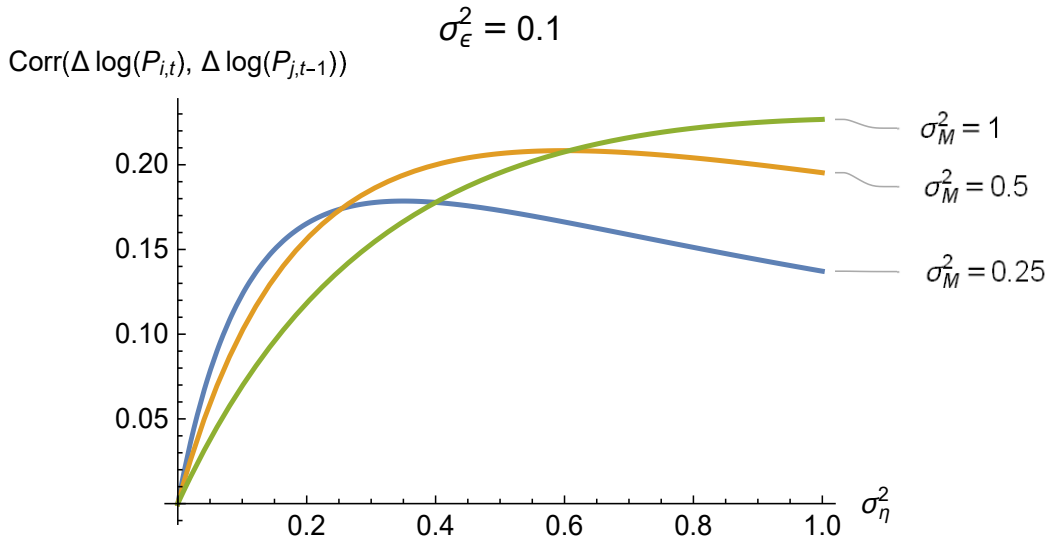
Figure 4: Cross-autocorrelation for different levels of disagreement (horizontal axis) and different levels of market volatility (different lines).
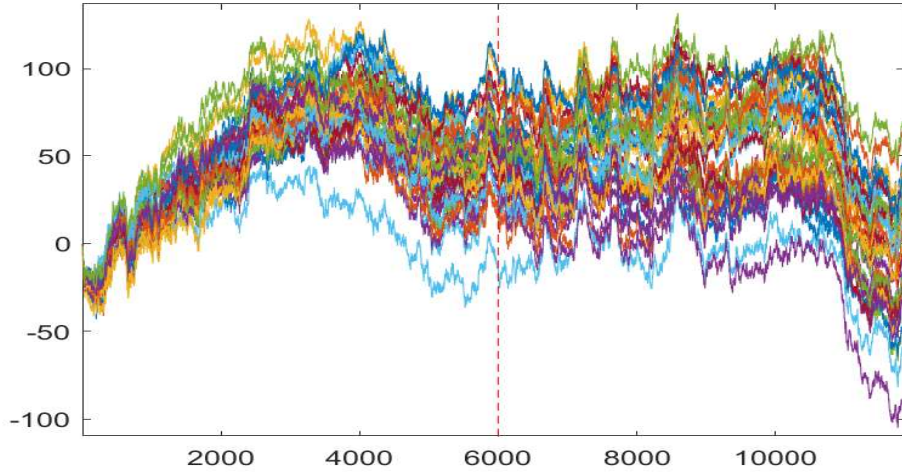
Figure 5: Logarithmic price data generated with $N = 40$ assets, by assuming $\sigma_M^2 = 1$, $\sigma_\epsilon^2 = 0.1$, $\sigma_\eta^2 = 0.1$ if $t < 6000$ and $\sigma_\eta^2 = 0.7$ if $t \geq 6000$. The vertical line indicates the time of the structural change.
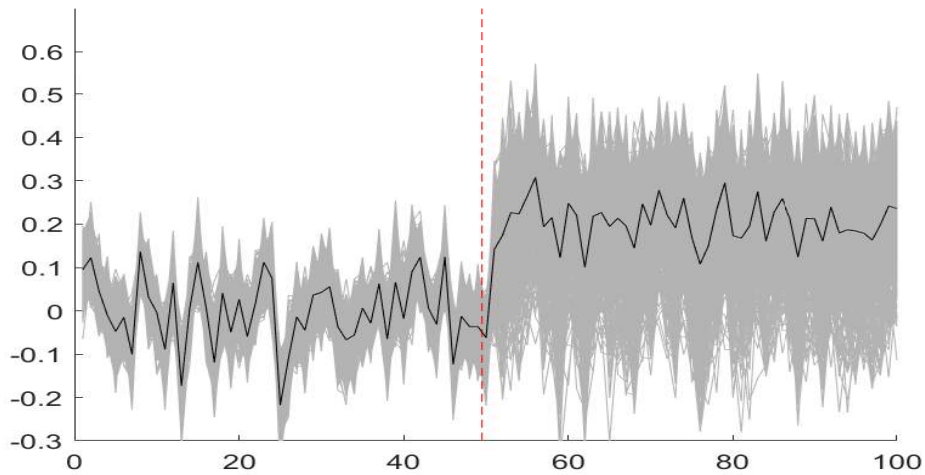
Figure 6: Estimated cross-autocorrelation value (gray lines) and average cross-autocorrelation (solid line) over 100 not overlapping windows of 120 observations each. The vertical line indicates the time of the structural change.
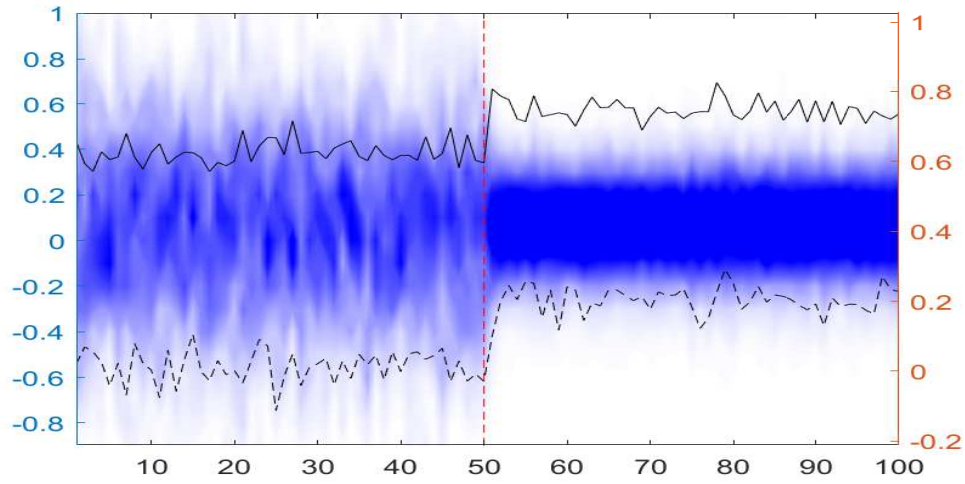
Figure 7: Estimated autoregressive coefficients (shaded blue area, left vertical axis), network density (dashed line, right vertical axis) and spectral radius (solid line, right vertical axis) over 100 not overlapping windows of 120 observations each. The vertical line indicates the time of the structural change.
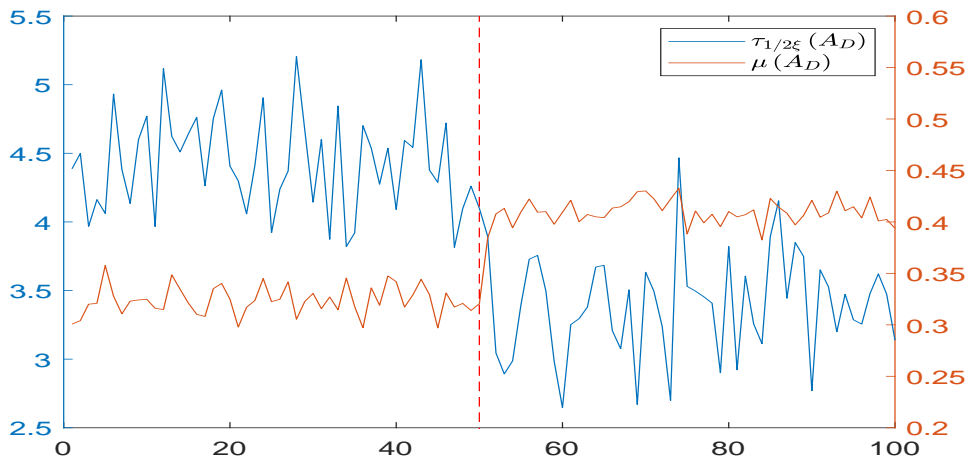

Figure 8: Estimated disagreement persistence $\tau_{\xi/2}(A_D)$ (left axis), and half-life disagreement $\mu(A_D)$ (right axis). The vertical line indicates the time of the structural change.
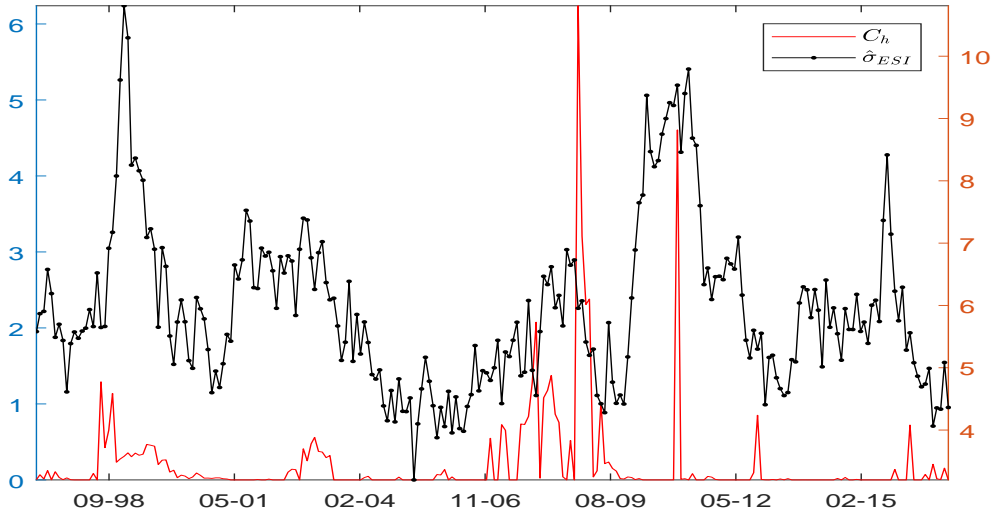
Figure 9: Total connectedness C_h on the left-scale and the cross-sectional standard deviation of national ESI indicators $\hat{\sigma}_{ESI}$ on the right-scale over the period 1996-2016.
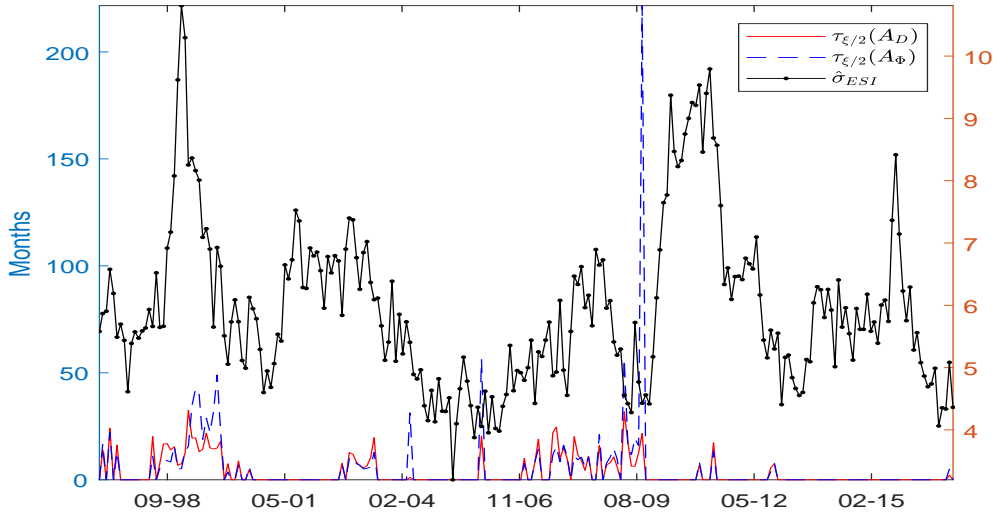

Figure 10: Half life of disagreement on connectedness ($\tau_{\xi/2}(A_D)$) and half life of disagreement on the forecast operator ($\tau_{\xi/2}(A_\Phi)$) on the left scale. On the right scale, the cross-sectional standard deviation of national ESI indicators($\hat{\sigma}_{ESI}$).
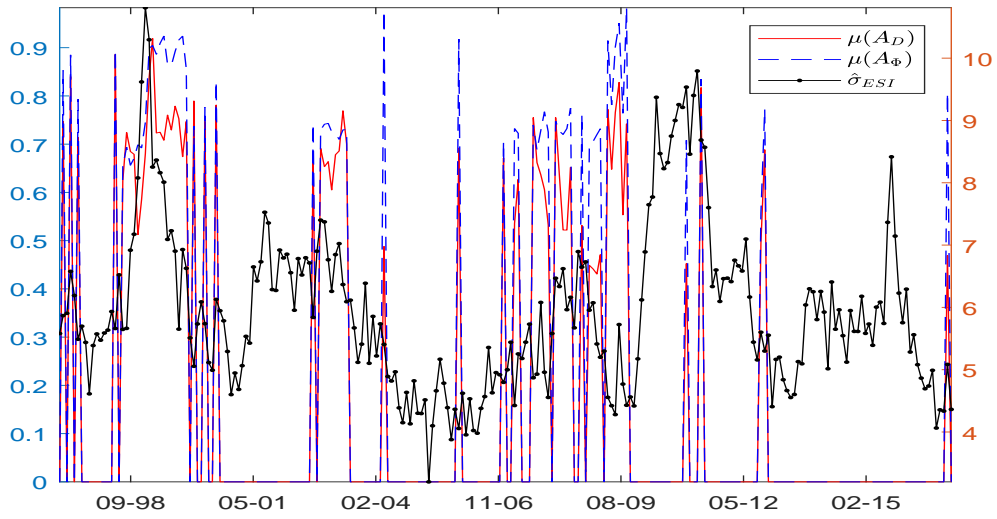
Figure 11: Disagreement persistence on connectedness ($\mu(A_D)$), the disagreement persistence on the forecast operator ($\mu(A_\Phi)$) and the cross-sectional standard deviation of national ESI indicators($\hat{\sigma}_{ESI}$).